Engineering Applications of Artificial Intelligence 137 (2024) 109173

Contents lists available at ScienceDirect

Engineering Applications of Artificial Intelligence

journal homepage: www.elsevier.com/locate/engappai

Detecting wheel slip from railway operational data through a combined wavelet, long short-term memory and neural network classification method

Bernadin Namoano [a], Christos Emmanouilidis [b,*], Andrew Starr [a]

[a] Cranfield University, School of Aerospace, Transport, and Manufacturing, UK
[b] University of Groningen, Department of Operations/ FEB, the Netherlands

ARTICLE INFO

Keywords:
Anomaly detection
Train wheel slip
Railway operations
Wavelet analysis
Long short term memory
Classification

ABSTRACT

— Detecting wheel slip is important in railway operations, to prevent damage to wheels and tracks, reduce maintenance costs, improve safety and enhance passenger comfort. Slip activity is characterised by reduced adhesion between the wheel and the rail and limits effective braking or acceleration, causing also operational risks. It is influenced by environmental conditions, vehicle load, track and axle quality, contaminants, inclines, rail oxidation, and braking forces. This paper introduces an innovative method for wheel slip detection in operational trains, utilizing wavelet analysis combined with Long-Short Term Memory (LSTM) modelling. This method analyzes operational data to effectively identify wheel slip, showing promising results when compared to traditional classification-based machine learning methods such as decision trees, forests, logistic regression, naïve Bayes, and support vector machines. This novel approach addresses the complexities of wheel slip detection and is capable of identifying the conditions leading to slip several seconds prior to the commencement of the slip event, offering a practical solution for real-world railway systems.

1. Introduction

Wheel slip activity poses substantial challenges in railway maintenance, with its most notable characteristic being diminished adhesion between the wheel and the rail, particularly during intense braking situations. This can negatively impact the integrity of both the rolling stock and tracks causing considerable safety risks. Negative impacts include reduced ability to stop; higher risk of signals passed at danger (SPAD) situations; ineffective acceleration or ability to travel at desired speed, causing longer journey duration; damage to train wheels and rails, leading to premature maintenance or replacement needs; and inability to initiate track circuit activation, with further severe safety implications (The Rail Delivery Group, 2018). Consequently, wheel slip activity can cause considerable maintenance costs, train delays, and safety or even accident risks, as severe defects can result in derailments. In addition, slippage between the wheel and rail can lead to a significant increase in temperature at the point of contact, potentially resulting in the softening of the materials involved (Yang et al., 2023). Further consequences include the acceleration of the growth of existing cracks in rails and nearby structures, as well as intensifying vibrations throughout the train, resulting in noise and discomfort for passengers Therefore, the development of wheel slip protection (WSP) mechanisms is vital not only for mitigating these adverse effects but also for prolonging the lifespan of associated assets.

WSP has been pursued via dedicated control systems, often making use of a range of sensing and actuating components. Such control systems may require analytical (Wu et al., 2023), simulation (Abouzeid et al., 2022), or numerical and finite element (Deng et al., 2022) modelling, including joint modelling approaches (Abouzeid et al., 2022; Lu et al., 2024). Their success depends much on the extent to which estimates or predictions derived from such modelling match the observed reality, but simulation-based approaches cannot fully account for the significant uncertainty around the real operational and surrounding environment conditions. Modelling approaches were in some cases combined with operational measurements to infer slip activity, with results validated under simulated data (Moaveni et al., 2020), via comparisons between simulated outcomes and limited field test data (Lu et al., 2024) or under controlled conditions in dedicated test rigs (Krummenacher et al., 2018) but wider testing and validation on extensive real operational situations was not reported. While WSP on modern trains benefits from such control systems, a large proportion of operational trains still have elementary protection which can still be

* Corresponding author.
E-mail address: c.emmanouilidis@rug.nl (C. Emmanouilidis).

https://doi.org/10.1016/j.engappai.2024.109173
Received 16 October 2023; Received in revised form 11 July 2024; Accepted 19 August 2024
Available online 30 August 2024
0952-1976/© 2024 The Authors. Published by Elsevier Ltd. This is an open access article under the CC BY license (http://creativecommons.org/licenses/by/4.0/).

upgraded via appropriate retrofitting hardware and data-driven solutions.

This paper presents the development of a wheel slip activity detection method based on operational data, which is capable of not only detecting slip events once they occurred, but also identifying early the onset of conditions leading to them, which is an improvement over current methods. It is applicable to the two main types of wheel slip, namely adhesion-limited and traction-limited slip. Adhesion limited slip occurs when the contact between the wheel and the rail is insufficient to transmit the required tractive or braking forces leading to wheel over-rotation (slippage). Traction-limited wheel slip is caused by excessive braking forces applied to the wheel, leading to a wheel lock (under-rotation). The proposed method is based on measurements which can be obtained from operational trains, namely brake pressures and train carriage axle speeds. It applies a combination of univariate axle speed analysis using a wavelet approach with a version of long short-term memory neural networks (LSTM) (Hochreiter and Schmidhuber, 1997), which fuses features extracted from the speed analysis wavelets with braking forces measurements. The method is shown to distinguish between normal and wheel slip conditions when tested on train operational measurements, showing a high level of accuracy compared to classification-based machine learning employing logistic regression, decision trees, random forests, k-nearest neighbours, and support vector machines. The analysis is conducted on several diesel multiple unit (DMU) trains' data from a whole year. An earlier version of this research with more limited experiments was reported in (Namoano et al., 2022). The main extensions here include (1) more extensive experiments, including a grid search for optimising numerical hyperparameters and more options for qualitative choices, providing a more extensive comparison basis for the research outcomes; (2) an updated methodology with a wavelet, LSTM and neural classification combined approach, with its description. Furthermore, a more in-depth analysis of both the targeted problem and related literature analysis is provided, and further insights are offered in relation to the obtained results, their limitations, and potential extensions of the work. The remainder of the paper is structured as follows. Section 2 offers an overview of related concepts and background literature. The developed methodology is presented in section 3. Comparative results are presented in section 4, including relevant discussion and recommendations. A conclusion is offered in section 5.

2. Problem background and related work

The modelling, detection, prediction, and control of slippage at the wheel-rail interface is a complex task due to the numerous factors influencing its occurrences, such as environmental conditions, overall vehicle load, track and axle quality, debris on rails, steep inclines, rail oxidation, and applied braking forces. To further explore the problem and position the presented research within the body of existing literature, the following sub-sections outline related concepts, introduce the problem of wheel slip activity, and analyse related works.

The employed abbreviations and notation are summarised in Table 1.

Table 1
Notation.

Symbol	Represents
WSP	Wheel slip protection
psi	Pound *per* square inch (pressure)
BCP_ax_{XX}	Brake Pressure measured over axle numbered XX in *psi*
Speed_ax{XX}	Speed measured over axle numbered XX
DMU	Diesel multiple unit
LSTM	Long short term memory (neural network)
Mph	Miles *per* hour (train speed)
GPS_speed	GPS-derived speed in mph
GPS	General positioning System

2.1. Related concepts and notation

The focus of the analysis is on DMU trains. A simplified DMU train is shown in Fig. 1. Each DMU train comprises three carriages, labelled as 64, 72, and 65, assuming a single middle carriage for simplification. The edge carriages are the leading ones and have their front axles (axles 1, 2, 11, and 12) powered. All middle carriages (marked here as a single carriage labelled 72) have the middle axles powered (6 and 7 axles in the figure). When braking, pressure is applied to the powered axles of all carriages. Wheel slip activity occurs mainly in the powered axles.

2.2. Wheel slip activity

Wheel slip can be categorised into two main types: traction-limited and adhesion-limited. Traction-limited slip is caused by excessive torque or braking forces applied to the wheel, leading to loss of grip and subsequent slip. It can result from equipment malfunctions, overly aggressive braking or acceleration, or uneven distribution of forces among the wheels. In general, traction limited slip can be corrected by power/brake control, and it is easier to detect when observing large braking forces in combination with erratic speed variability, as seen in Fig. 2. In the figure, the travel profile includes three phases: two stoppage segments and one travel segment. After initial stoppage, the train accelerated until it reached about 50 mph. After time [70] intense braking is applied with braking pressure reaching a maximum level (i.e., above 3 psi for both axles) resulting in the speeds at Ax1 (front axle) and Ax12 not being well aligned anymore, indicating locked wheels slip events. This triggers reduction in braking pressure until eventually the train is brought to a stop.

Conversely, adhesion-limited slip is harder to detect from axle speed and braking pressure profiles. Adhesion-limited slip occurs when the adhesion between the wheel and the rail is insufficient to transmit the required tractive or braking forces. It is often caused by external factors such as wet or icy rail conditions, rail contamination, or wheel-rail geometry issues, such as out of roundness conditions (OOR or flat spots) (Maglio et al., 2022). For example, Fig. 3 shows an example from an experimental test on a train journey with poor track quality, which includes a sequence of flat spots in the rail surface, causing the erratic speed profile between [40–60], which does not coincide with braking, but it is an adhesion-limited case. However, no association of this erratic behaviour can be made with intense braking as, in contrast to the traction-limited case of Fig. 2, there are no braking events during the slip and so it can easily be left uncorrected, unless it is properly detected. Note that moderate braking events after time [80] do not cause slip and are not associated with erratic speed patterns. Given the challenges of adhesion-limited slip, the interest in the present work is greater in adhesion limited slip, seeking to explore the extent to which detection, preferably with early warning, is feasible.

Overall, in both traction-limited and adhesion-limited cases, OOR defects on wheels and rails are significant contributors to slip phenomena. They can lead to more uneven wheel-rail interface, reducing traction, even without intense breaking and accelerating, which can also be exacerbated through increased vibration. Due to the wide range of factors affecting the wheel-rail interface, modelling the underlying phenomena and applying WSP are not straightforward, as discussed next.

2.3. Wheel – rail interface modelling and wheel slip protection

Investigating the wheel-rail interaction has been the focus of much attention in seeking to comprehend wheel slip phenomena. When vehicles accelerate, the rotational forces applied on the axles are amplified, but when the frictional or rolling resistance between the wheel and rail doesn't meet the force induced by the escalated torque, it leads to over-rotation or wheel slip activity. Furthermore, under braking conditions, the wheels can under-rotate. Then, the braking force, acting as

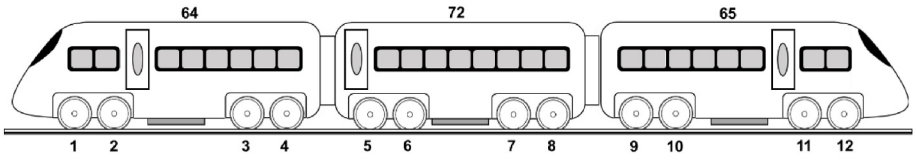

Fig. 1. Diesel Multiple Unit train and powered axles.

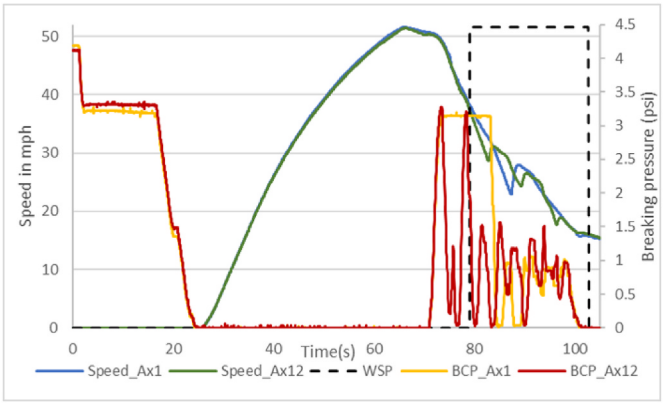

Fig. 2. Traction limited slip: wheel lock causing wheel slip activity.

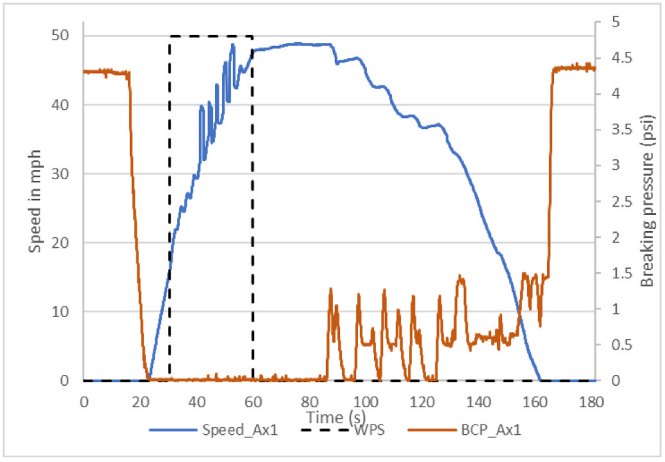

Fig. 3. Adhesion – limited slip: rail track flat spot defect causing slip.

resistance, counters the rotational force from the torque under traction. When the braking force exceeds the wheels resistive force on the rail track, it results in the wheel lock-up, thus potentially causing flat spots. These spots pose significant risks as the resulting repetitive impact can damage the wheel and the rail. While small slip events may go unnoticed and are often of little concern, excessive slip may inflict damage to the rail and wheels (Enblom, 2009) and needs to be prevented.

The investigation of wheel slip activity has been conducted via analysis of adhesion conditions between wheels and rail tracks (Iwnicki, 2006). In analytical modelling approaches, the ratio of longitudinal to normal forces is represented by the coefficient of adhesion. Adhesion coefficients need to adhere to a set of safety standards (UIC, 2005) across all the different rail track segments. However, factors such as contamination by substances like oil, snow, grease, water, leaves, wear products, oxides, ballasts, and dust on wheel-rail interfaces significantly affect this coefficient (Bosso et al., 2019; Wu et al., 2023). Producers of components such as braking systems, wheels, and rails ensure their products undergo a variety of tests under differing conditions of wear and tear, in order to meet the stipulated standards (UIC, 2005; Barna, 2011). Typically, this analysis is conducted offline and is driven by models that simulate vehicle dynamics, such as braking distance, range of vehicle velocity, wheel lock limit or slide limit, and air pressure in the braking system (Barna, 2011). Further analysis has been reported on improving adhesion by examining the impact of contaminants (Lewis and Olofsson, 2009; Garnham and Davis, 2009).

To minimise time and expenses related to experimental work on wheel slip protection, existing guidelines such as those specified in (EN 15595, 2021) allow for hardware in the loop (HIL) simulations (Yin et al., 2024), although there are restrictions regarding HIL usage. Testing setups are divided into four distinct levels of complexity (levels 1, 2a, 2b, and 3). Level 1 refers to a basic WSP system, and often uses modulation of the brake application. Level 2a is more advanced and has better time response than level 1. Level 2b is more advanced than 2a and incorporates slippage prediction. Level 3 is the most advanced WSP system and integrates with other carriage control systems as a holistic approach to improve vehicle dynamics and safety. Standards (EN 15595, 2021) (UIC, 2005) also lay out requirements for HIL testing. The design guidelines for testing rigs were first introduced by BR-AEA tech in the late 1990s (Nicks, 1998). More recently a hybrid simulator base method was employed for WSP performance evaluation (Ishige, 2021), while a bench test was employed to simulate the air compressed pressure in the vehicle brakes (Hijkata et al., 2021). The simulated pressure is used to investigate WSP performance. While the simulation can capture realistic behaviour, it is still limited compared to the specific dynamics of a real environment. Other approaches seek to estimate the damage inflicted on railway carriage wheels by lock-up braking (Krénusz et al., 2021), showing through simulations that even when meeting UIC requirements and with WSP operating correctly, small damage can still occur on the rail-wheel contact. Therefore, continuous monitoring and validation of WSP is needed as investigated on a test rig (Pugi et al., 2023). While experimental results have shown high accuracy, assumptions such as constant vehicle mass, speed, and friction coefficients do not always hold in operational settings. In addition, these models may involve numerous parameters, making them hard to reliably estimate in such operational settings. Therefore, model-driven methods have limitations when applied to real-world applications.

WSP has been the focus of several studies which reported the development of dedicated control systems. While such control systems are increasingly equipping newly manufactured trains, a large proportion of currently operating trains are equipped with basic only protection mechanisms and retrofitting legacy systems with such mechanisms is complex. Control systems may follow a combination of analytical and simulation modelling to derive appropriate torque control, to ensure torque demand is dynamically met by the actual torque of the driving forces, and adhesion control, seeking to control the tractive and braking forces, preventing wheel slip (Abouzeid et al., 2022). In another approach, numerical analysis via finite element modelling is employed to study the wheel-rail interface phenomena (Deng et al., 2022), providing theoretical guidance for the development of more accurate control methods of wheel slips. Brake modelling can also be employed to understand the wheel-rail adhesion and its impact on wheel slip (Wu et al., 2023). However, in both previous works, success depends much on the extent that such estimates and analytical modelling match the observed reality and simulation-based – approaches cannot account for the significant uncertainty around the real operational conditions. Alternatively, measurements from the train's drive motor current can be

translated into estimates for the wheel speed and the train's longitudinal velocity, which in turn can be analytically processed for short term wheel slip prediction. Such prediction can feed into a model predictive wheel slip control approach (Moaveni et al., 2020). However, other studies reported that single predictive model approaches are potentially insufficient, as any combination of changes in the factors affecting or contributing to wheel slip activity may render the model inadequate, and therefore an approach which seeks to employ multiple candidate models has also been proposed (Zirek and Onat, 2020). The development was tested and validated under controlled conditions in dedicated test rigs but wider testing and validation on extensive real operational situations was not reported. However, detection of wheel slip activity needs to be developed, tested and validated in more extensive and wide-ranging operational situations and this remains a challenge for trains without pre-installed advanced control mechanisms, requiring retrofitting with more advanced solutions. In one such work, measurements relevant to the wheel-rail interface are taken by installing wheel load checkpoints through strain gauges installed on rails (Krummenacher et al., 2018). In this work, to account for the transient phenomena of the wheel-rail interface, wavelet analysis was performed to extract potentially informative features. These resulted in datasets which were annotated by reprofiling the original data with events, as assumed by examining protocols of repair workshop of freight trains and regular maintenance measurements of passenger trains. The annotated datasets were then fed into a machine learning model employing support vector machines to detect wheel slip. Such reprofiling inevitably brings uncertainty regarding the precision of the annotation. Furthermore, instead of focusing on the rolling stock where the actual wheel slip originates, the developed method targets the apparent indirect observation of any observed slip activity on the fixed asset infrastructure, and therefore is more susceptible to other unmodelled phenomena or noise.

Wheel slip control uses wheel slip quantification, such as the wheel slip ratio, λ defined as:

$$\lambda = \frac{\boldsymbol{\omega_r} * R - V}{\boldsymbol{max}(\boldsymbol{\omega_r} * R, V)}$$

where $\boldsymbol{\omega_r}$ is the angular speed of the wheel, $\boldsymbol{R}$ is the effective wheel radius, and $\boldsymbol{V}$ is the linear speed of the vehicle. The wheel slip ratio can take values from -1 (indicating full braking slip) to $+1$ (indicating full traction slip), with 0 representing no slip. The principle of an anti-slip controller is to trigger corrective actions (for example applying sanding) when the slip ratio exceeds certain thresholds, which might be different for acceleration (positive slip) and braking (negative slip). Older trains where not equipped with WSP mechanisms and relied more on driver's expertise during operation, or on experienced technicians and engineers during maintenance. Increasingly, trains were retrofitted with WSP mechanisms (e.g. sanding, control systems for power/braking/traction). Such mechanisms are commonly used in modern trains, but legacy ones still lack them and there is a need to apply condition monitoring at the wheel-rail interface to detect wheel slip given the challenges of analytical modelling (Charles et al., 2008). However, in practice, triggering WSP based on pre-determined λ values and thresholds, might not be as effective as relying on real observed behaviour, and so an attractive alternative would be to apply a gradient detector of changes, which can be learned from data. Overall, in related works, testing and validation is largely performed over simulated data and when real life measurements were involved, these were taken under controlled conditions in dedicated test rigs, or from the permanent way of the railway infrastructure, or in a limited way from rolling stock measurements to derive analytical estimates to feed into predictive controls. Wider testing and validation on extensive real operational situations remain scarce. Therefore, data-driven approaches for slippage detection are still needed, which can be driven by real-world operational data which can be made available and utilised to this end.

3. Methodology

The aim of the present work is to develop a data-driven approach for wheel slip detection applicable to everyday operational settings. The overall data processing workflow is illustrated in Fig. 4 and comprises data acquisition, preprocessing, features extraction, model building, and model performance assessment, with each stage presented next.

3.1. Stage 1: data acquisition

Urban trains, operating under varying conditions and across diverse geographical locations, serve as the data source for this research. The operational measurement logs comprise one year of measurements from the daily operation of four operational trains on the same railway track. These are approximately 160,000 datasets in total. Each dataset comprises time series of measurements taken across the three carriages of the train equipped with measurement sensors. The recorded data include a timestamp, GPS coordinates, GPS-derived train speed, axle speeds, braking pressures and mechanisms, additional measurements from accelerometers, and axles sanding levels. The datasets were further annotated with wheel slip events from each one of the three monitored carriages. Any slip in one of the three such carriages would be marked as an overall slip event. A sampling rate of 20Hz is employed. Although such a rate can be insufficient at times in detecting the occurrence or the development of defects, it is nonetheless sufficient for capturing slippage phenomena, preventing the omission of any significant events, according to industry practice in this domain. Axle numbering is as in Fig. 1, with axles 1, 2, 6, 7, 11, and 12 being the powered ones.

3.2. Stage 2: pre-processing

Stage 2 is the pre-processing stage and involves smoothing, time alignment, and segmentation.

Filtering: The train movements induce disturbances that typically accompany the braking and speed signals. To reduce these disturbances and improve signal quality, low-pass filtering in the form of an exponential moving average with a window of five time steps was applied. The rationale behind choosing this specific window size is based on the nature of the process being monitored. Given the dynamics of the train movement and the nature of the signals being observed, a time granularity of 0.25 s has been empirically identified as appropriate for each time step (more on this in section 3.3). It provides a balance between smoothing out noise and retaining the essence of the signal pattern, thus

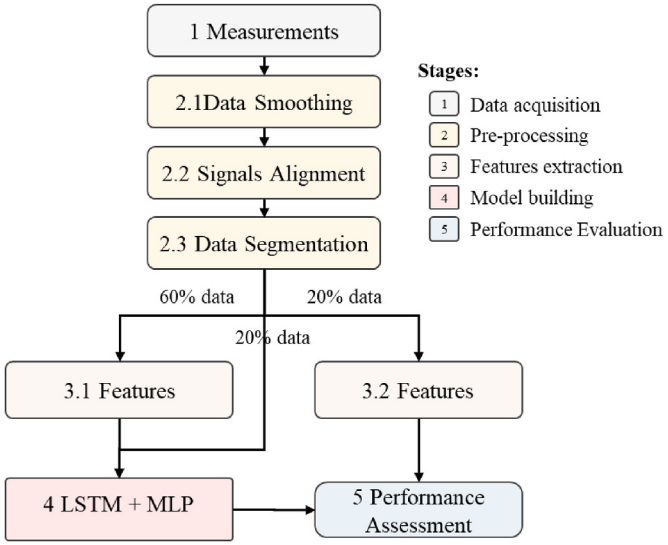

Fig. 4. Wheel-rail interface data processing workflow.

allowing for a more accurate representation of the process.

Time alignment: As collected data are from various locations, desynchronization and time lags between the signals are often observed. These phenomena necessitate the establishment of robust data alignment methods for the extracted data to be used for computational processes, including machine learning. Initial alignment is accomplished through the synchronization of the GPS time as recorded with the time logged by the train's axle sensors. This process constitutes the first step of alignment. Note that an overall wheel slip event may arise from any of the three monitored carriages, therefore a single slip event in any of these carriages is enough to mark a specific record as corresponding to a slip event. For this reason, data synchronisation needs to be performed with high accuracy. Therefore, following the first alignment step, a secondary alignment step is implemented. This involves employing Dynamic Time Wrapping (DTW), as implemented by (Keogh and Ratanamahatana, 2005), using the L2-norm as a distance metric to align the data. DTW is a computational technique that provides an efficient and effective solution for aligning sequences with similarity. Through the application of this two-tiered time alignment procedure, the data sequences derived from the streaming data are adjusted to achieve a high level of temporal synchronization. It ensures the minimization of errors or discrepancies due to time lag or desynchronization, enhancing the accuracy and reliability of subsequent modelling and machine learning activities.

Segmentation: After improving the quality of the data, segmentation is performed to divide it into shorter time series segments, each one constituting a train journey between two stations. For clarity, a train journey is described as the continuous progression of a train from its departure at one station until it reaches and halts at the next station. To perform effective and accurate segmentation, several sensor measurements are considered, including axle speed, brake pressure and GPS coordinates. The first type of measurement is axle speed. For a segment to be recorded, the speed of the axles must decrease to zero and maintain this state for a period more than 2 min. This specific duration was chosen based on the expert advice of domain specialists. They argued this duration is typically the minimum normal stop duration time. However, segmentation doesn't rely solely on axle speeds. It also employs the brake pressures measurement to validate that the driver has stopped as the brake pressure will increase to a high maximum level. The first two measurements guarantee that the train stopped but not necessarily at a train station or depot. Hence, the next measurement involves binary records on the actions of the train's doors, and whether they are unlocking, opening, or closing. Through the integration of these attributes, a heuristic rule, such as "if the train doors are open and the halt exceeds 2 min, the train is at a station" is applied as the overall segmentation rule. To enhance the precision of this approach, the train GPS coordinates are utilised to compute the distance between the train's current location and the closest station. For a scenario to be classified as the train being at a station, this distance must be within an empirically determined threshold, set to 200 m. The threshold is also from the expert advice as the leading carriage can influence the GPS location at the stopping stations. Data-driven processing without contextualisation is a harder task. Employing contextualisation heuristic rules and considering both axle speeds and door activity events, steers the segmentation process, by grounding it to domain-specific knowledge, thereby empowering stakeholders to make better informed data-driven decisions. At the end, each time series segment is a sequence of time-stamped multivariate data records, with the following attributes:

Input attributes: Sequences of data records of the following type, for each segment [Time stamping, BCP_ax_1, BCP_ax_2, BCP_ax_6, BCP_ax_7, BCP_ax_11, BCP_ax_12, Speed_ax1, Speed_ax2, Speed_ax6, Speed_ax7, Speed_ax11, Speed_ax12, GPS_Speed].

Outputs (Ground truth): Sequences of binary data for each carriage, indicating that a current measurement corresponds or not to wheel slip: [Wheel Slip: 1 if event is true; 0 if event is not true] Other attributes which contributed to pre-processing, are not employed further.

3.3. Stage 3 feature extraction

To capture transient patterns in the axle speed values, which are likely to be the result of wheel slip, gradient features are derived from axle speed profiles through the angular function (t) :

$$\varphi(t) = \tan^{-1}\frac{Y_{t+k} - Y_t}{X_{t+k} - X_t} \tag{1}$$

where tan^{-1} is the inverse tangent function, Y_t represents the axle speed at time t, and X_t represents the time instance. To account for error quantization and handle noise, the k value is set to 5 and each time step is 0.25 s. Obtained data were labelled as normal or faulty by industry experts, thereby including domain knowledge in the process. Specifically, annotation was validated by experts using the absolute difference of front axle 1 (located in the first carriage) and back axle 12 (located in the third carriage), applying a rule of thumb that a difference above 0.8 mph is considered as wheel slip. Wheel slips represent a fast transition between normal to slip conditions within short time periods and transient phenomena can be captured by wavelet analysis. A basis function ψ is a wavelet, also known as a mother wavelet, if it satisfies the admissibility condition:

$$\int_{-\infty}^{+\infty} \frac{|\widetilde{\psi}(w)|}{|w|} \mathrm{d}w < \infty \tag{2}$$

where $\widetilde{\Psi}$ is the Fourier transform of ψ. Many wavelets have been proposed over time, for example, Haar, Daubechies, Gaussian, and Morlet wavelets (Misiti et al., 2006). They differ from each other by their vanishing moments, which give different local regularities. The Morlet wavelet is used in the context of the present work, as it was seen to relate well with how human vision operates (Daugman, 1985). The scaling (dilatation) of the wavelet ψ with a factor α is defined as follows:

$$\psi_t(t) = \frac{1}{\alpha}\psi\left(\frac{t}{\alpha}\right) \tag{3}$$

The wavelet transform of a signal S is denoted by C and for finite energy, at the scale (dilation) α at time t is defined by:

$$C(\alpha, t) = S(t) * \psi_\alpha(t) \tag{4}$$

where * is the convolution operation. The coefficients $C(\alpha, t)$ measure the variations of the signal S at the dilatation α. Brake pressures and axles pressures are used as S during the analysis. From a qualitative point of view, large $C(\alpha, t)$ values indicate irregularity of the signal S around the position t at the dilatation α. Conversely, small values of the coefficients indicate signal regularity. Therefore, they are likely to convey information about slip phenomena. The sequences of these coefficients are then used as inputs to the next step for extended features learning and fault classification.

3.4. Stage 3 model building

The final analysis stage involves multivariate joint LSTM and MLP learning for wheel slip detection, which is described in more detail here. After obtaining signals improved quality and features which are likely to be informative, the next problem is to capture the signal dynamics, while keeping a good balance of modelling both short and longer-term phenomena. Conventional feed-forward networks fail to explicitly incorporate prior predicted outputs, thereby likely missing short-term dependencies. Various types of recurrent neural networks (RNNs), including those reported in (Lukoševičius and Jaeger, 2009) were designed to address this issue by introducing a feedback loop between network layers, thereby enabling sequential learning. However, they struggle with long-term dependency learning due to the complications of exploding and vanishing gradients (Pascanu et al., 2012). LSTM networks (Hochreiter and Schmidhuber, 1997) were developed to tackle

these challenges. These networks effectively prevent gradients from either growing infinitely (exploding) or decaying to insignificance (vanishing). This is achieved by introducing "cell" and "gate" structures, which guide the selection of gradient updates, into the conventional neural network architecture. The application of LSTM methodologies to wheel slip activity detection is justified by the inherent time lag between causative factors (e.g., hard braking, track condition) and the resulting observable outputs. Furthermore, wheel slips can cause damage, leading to intermittent faults. Therefore, both short-term and long-term phenomena may influence the final model outcome. Additionally, the ability of LSTM networks to manage multivariate attributes exhibiting complex non-linear relationships aligns well with the requirements of the problem at hand. Therefore, LSTM modelling is applied for extended features extraction. One LSTM is built for each one of the input signals (brake pressures, axles speeds, GPS speed) and their outputs are then jointly fed into a simple MLP classification model for slip detection. The earlier described wavelet analysis has already been employed to identify rapid signal changes.

3.5. Performance assessment

Given the nature of the detection activity, performance metrics for classification are applied. These are precision (P), recall (R), and the F1_score $F1$. Precision quantifies the percentage of real wheel slip cases which are included in the detected ones. Recall quantifies the percentage of wheel slip cases identified as such. The F1-score is the harmonic mean of the precision and recall. It is beneficial when dealing with unequal distribution of classes or when the significance of false positives and false negatives diverge in a particular scenario. The metrics are as follows.

$$Precision(P) = \frac{Number\ of\ correctly\ predicted\ wheel\ slippage\ cases}{Number\ of\ wheel\ slippage\ predicted\ (correct\ or\ not)}\ \text{x100} \tag{5}$$

$$Recall\ (R) = \frac{Number\ of\ correctly\ predicted\ wheel\ slippage}{Number\ of\ wheel\ slippage}\text{x100} \tag{6}$$

$$F1_score(F1) = 2\frac{P.R}{P+R} \tag{7}$$

3.6. Design of experiments

The experimental process of this study utilised real-world data, provided by an industrial collaborator. The dataset comprises records of approximately 160,000 observations. These cover a one-year period of urban train operations. The hyper-parameters for each method are seen in Table 2, including settings for a grid search aimed at identified specific combinations of hyperparameters which deliver better performance for each method. The data was partitioned into training, testing, and validation sets, at a percentage of 60%/20%/20% respectively. Given the time series nature of the problem, the partitioning was applied to choose a percentage of time series segments, rather that splitting the data of individual segments. The LSTM was implemented using the relevant using Keras and TensorFlow libraries. To validate the effectiveness of the of methodology, a comparison is made with other machine learning options.

Decision tree: (i) *Maximum Depth of the Tree*: A tree with a greater depth will be more complex and could lead to overfitting of the data. A tree with a lower depth could lead to underfitting. (ii*) Minimum Samples Split*: This refers to the minimum number of samples required to split an internal node. (iii) *Minimum number of instances per leaf*: This is the minimum number of samples required to be at a leaf node. A smaller number makes the model more prone to capturing data noise.

K-Nearest Neighbours (KNN): (i) *Number of Neighbours*: It determines the number of nearest neighbours that will vote for the class or determine the value of the unknown point. (ii) *Distance Measure*: The distance measure is used to identify the "closest" points. (ii) The algorithm used to compute the nearest neighbours. Options include 'brute' (brute-force search), 'ball_tree', 'kd_tree', or 'auto' (which attempts to decide the most appropriate algorithm).

Naive Bayes: No parameter was used for Bayesian classification.

Support ***Vector Machines (SVM)***: Key tuning parameters in SVM include: (i) *Cost* (Regularization) parameter: The cost parameter trades off correct classification of training examples against maximization of the decision function's margin. (ii) *Kernel*: It determines the type of hyperplane used to separate the data. It can be 'linear', 'poly', 'rbf', 'sigmoid', or 'precomputed'. It defines the kernel function to be used in the algorithm, enabling SVM to create non-linear classifiers. (iii) *Numerical tolerance*: This defines the influence of a single training example, with low values meaning 'far' and high values meaning 'close'. It can be 'scale', 'auto', or a float.

Table 2
Design of experiments and relevant parameters.

	Parameters	Training
Data	**Total number of datasets**: 160,000 **Training datasets**: 96,000 **Testing datasets**: 32,000 **Validation**: 32,000 **Number of attributes**: 13 **Input signals**: axle speeds, brake pressures **Output**: ground truth of slip events	**N/A**
MLP following Wavelet + LSTM	**Mother wavelet:** Morlet **Hidden neurons per layer**: 50, 90,60 **Activation**: ReLU, sigmoid, sigmoid **Solver**: m-adam **Dropout parameter**: 0.05	**N/A** Empirical testing on different number of hidden layers and neurons for each layer.
Decision trees	**Minimum number of instances per leave:** 50 **Maximal tree depth:** 1000 **Minimum samples split:** 80	**SearchMethod**: GridSearchCV **Number of instances per leave**: [1; 1000] step of 1
K-NN	**Number of neighbours:** 50 **Metric:** Mahalanobis **Weight:** Uniform weight **Algorithm:** Euclidian	**SearchMethod**: GridSearchCV **Number of neighbours**: [1; 1000], step of 1 **Distance**: Euclidian, Mahalanobis **Scoring**: f1-score
Naive Bayes	**N/A**	**N/A**
Logistic regression	**Regularization:** Ridge (L2-norm)	Training with lasso and ridge regression. Grid search from [0.001; 1000], step of 10
SVM	**C:** 1.00 **Kernel:** Radial Basis Function (RBF) **Gamma:** 0.001	**SearchMethod**: GridSearchCV **Gamma**: [0.001; 1000], step: 0.01 **C**: [-2; 2] with a step of 0.1. **Scoring**: f1-score **Tested Kernels**: Linear: Polynomial: g: range [0; 10], step 0.01 c: range [0; 10], step 0.01 d: range [0; 10], step 0.01 RBF g: range [0; 10], step 0.01 Sigmoid g: range [0; 10], step 0.01 c: range [0; 10], step 0.01
Random forest	**Number of trees:** 80 **Maximal tree depth:** 1000 **Minimum samples split:** 70	**SearchMethod**: GridSearchCV **Number of trees**: [1; 1000], step of 1 **Scoring**: f1-score

Random Forest implements ensemble learning with multiple decision trees. When applied with "Random Subspaces" and "Bootstrap Aggregating", it takes the form of bagging.

Logistic regression: The key tuning parameters is the Cost penalty (Regularization type).

MLP (following wavelet + LSTM): Key tuning parameters include: (i) *Number of Hidden Layers;* (ii) *Hidden neurons per layer;* (iii) *Batch Size;* The number of samples propagated through the network before updating the model parameters. (iv) *Number of Epochs*: The number of times the learning algorithm works through the entire training dataset. (v) *Dropout parameter*: The dropout sets the ratio of randomly selected neurons to be ignored during training. (vii) *Optimizer*: The learning method used to adapt network weights and learning rate, to optimise the loss function.

Overall, the methodology of the data-driven wheel slip detection approach, illustrated in Fig. 4, included data acquisition, preprocessing through data filtering, time alignment, and time series segmentation, followed by feature extraction, model building, and model performance assessment. The next section presents the obtained results from applying the proposed methodology.

4. Results

This section presents the results of the experiments introduced in section 3. Specifically, results are first presented for traction – limited and then for adhesion-limited slip. To aid the interpretation of the obtained results, a discussion section is included, employing examples from each type of slip. Finally, the limitations of the study are outlined, pointing to issues open to further research. In the methods which involved a grid search for hyperparameters, performance is reported from applying models with the best settings identified via the grid search. Performance is reported in terms of F1 score, precision and recall, which are standard classification performance metrics.

4.1. Results

The performance of the methods in detecting traction – limited slip is presented in Table 3.

Under traction-limited conditions, the slip detection appears to be successfully performed by several of the employed models, as evidenced by the presented classification metrics F1, Precision, and Recall. The Random Forest model emerges as the top performer, achieving an F1 score of 99.41%, with matching precision and recall metrics (99.41% and 99.40%, respectively). This is evidence of successfully detecting traction – limited wheel slip. However, slip in adhesion-limited conditions is more challenges. This is shown in Table 4, with lower performance achieved by most approaches. The exception is the LSTM + MLP model, which significantly outperforms all other models with a high F1 score of 99.94%, demonstrating high precision (99.84%) and recall (99.43%).

Focusing on the LSTM + MLP approach, it is of interest to examine in more detail cases of imperfect wheel slip detection. On the evidence that adhesion-limited slip is harder to detect compared to traction-limited cases, adhesion-limited slip cases are chosen first. To aid with the interpretation of the results, the wheel slip activity is illustrated together

Table 3
Traction limited Validation results of the classification models in percentages.

Model	F1	Precision	Recall
DecisionTree	99.29%	99.29%	99.29%
kNN	98.46%	98.48%	98.45%
Naive Bayes	96.20%	96.20%	96.19%
Logistic Regression	79.76%	80.86%	78.69%
SVM	97.20%	97.25%	97.14%
Random Forest	99.41%	99.41%	99.40%
LSTM + MLP	99.28%	99.37%	99.19%

Table 4
Adhesion limited Validation results of the classification models in percentages.

Model	F1	Precision	Recall
Decision Tree	92.18%	92.05%	92.31%
kNN	93.57%	93.68%	93.46%
Naive Bayes	80.91%	80.37%	81.46%
Logistic Regression	61.08%	60.69%	61.47%
SVM	80.28%	83.42%	77.37%
Random Forest	93.19%	93.08%	93.30%
LSTM + MLP	99.63%	99.84%	99.43%

with the corresponding axle 1 and 12 speeds. No braking pressure is applied in these cases (orange coloured line in the figures), and, therefore, slip phenomena cannot be associated with braking. In Fig. 5, wheel slip activity is clearly evident from time 1.4 onwards, with the two axle speeds diverging. However, signs of wheel slip are evident earlier, with lower intensity events at around time 0.5 and 0.8. The onboard system marks the start of the wheel slip activity at around time 1. However, the LSTM + MLP approach achieves to detect slip events earlier, coinciding with these lower intensity events. They both continue to flag the conditions as corresponding to wheel slip when the two axle slips differ significantly, but the LSTM + MLP approach achieves an earlier detection.

Fig. 6 is a case of wheel slip commencing early in the shown time window. Again, the LSTM + MLP approach achieves an earlier detection compared to the onboard system. The condition is a continuous case of wheel slip, although the onboard system registers this as two separate slip events, separated by a non-slip short duration. In both cases the LSTM + MLP approach is clearly an improvement over the onboard system.

Figs. 7 and 8 show cases of traction-limited slip. In these cases, braking pressure is a significant contributor to wheel slip, and the pressure is shown with orange colour. In Fig. 7, wheel slip events can be recognised already before time 1 with several such events thereafter. The first slip event coincides with a peak in braking pressure. As in the previous case, the LSTM + MLP detects the slip earlier than the onboard system. Any divergence between the axle speeds has a much shorter duration compared to the adhesion limited case indicating slip events of lower impact on the smoothness of the carriage's movement. The LSTM + MLP appears to detect them with a higher sensitivity and at higher resolution (multiple events) compared to the onboard system, which registers a single continuous slip event. Fig. 8 illustrates the situation of a gradual increase in braking pressure. Here, the onboard system misses to register the slip at about time 0.25, which is nonetheless successfully detected by the LSTM + MLP approach. The onboard system eventually registers the slip at about time 1. This is also registered by the LSTM +

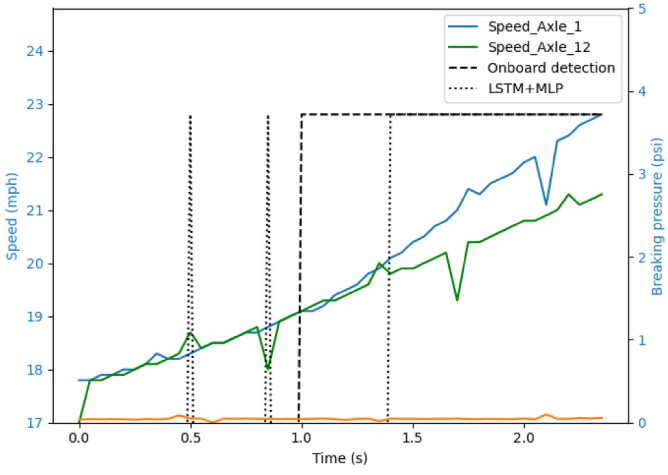

Fig. 5. Example of adhesion limited wheel slip.

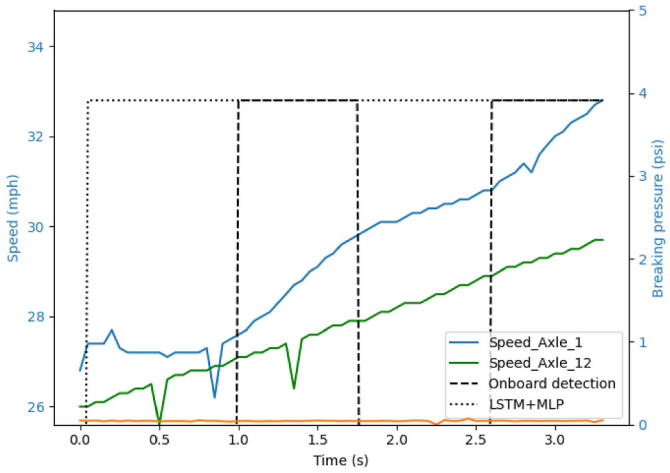

Fig. 6. Example of adhesion limited wheel slip.

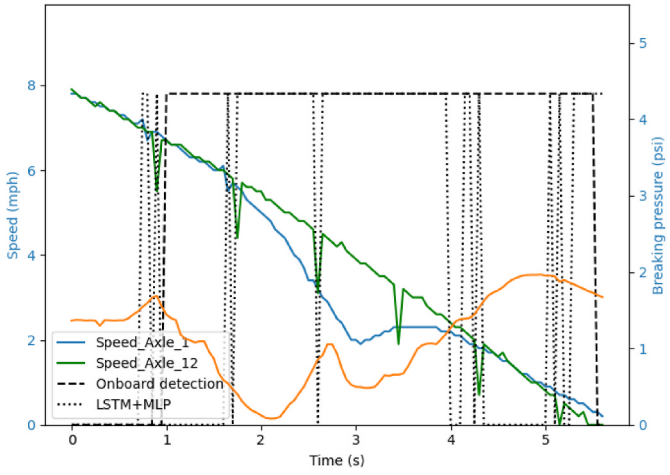

Fig. 7. Example of traction limited wheel slip.

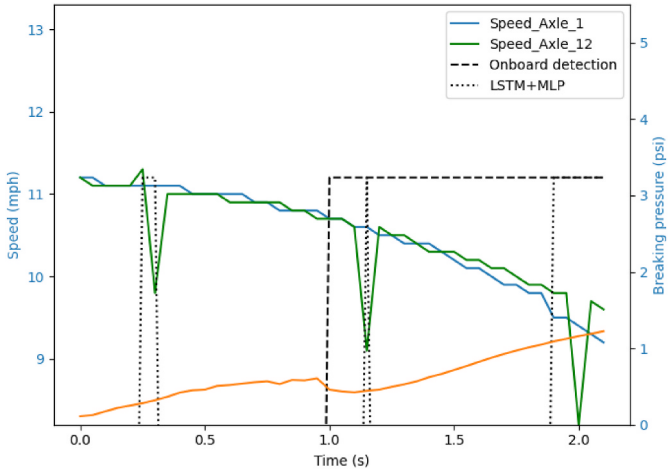

Fig. 8. Example of traction limited wheel slip.

MLP approach, albeit with more precision, as occurring at about time 1.1. The movement shows fewer abrupt fluctuations compared to the previous case, yet the LSTM + MLP approach appears to detect them with more prevision, as it additionally registers the one occurring at about 1.9 as a continuous slip event.

A case of slip detection during the acceleration phase is shown in Fig. 9. Here the train speed increases gradually, with the acceleration becoming somewhat steeper after about time 22. The two axle speeds diverge soon after, during a long slip event, briefly converge between about time 55 and 60 and diverge again. The LSTM + MLP approach is again able to detect the slip phenomena. It is noticeable that this is an early detection, which is particularly valuable. This demonstrates that the developed detection approach could be a valuable addition to onboard detection systems, as the experiments performed provided evidence of earlier and more accurate detection compared to onboard systems. Interestingly, in cases such as those of Fig. 9, the early timing of the detection could be linked to the causal relationship between the applied braking and acceleration, and the slip, without nonetheless resulting in false detections, i.e. braking and acceleration without slip.

4.2. Discussion

This paper presented a data-driven approach for wheel slip detection based on the combined use of LSTM and MLP networks. The developed approach was tested on real data from operational trains, providing evidence of high detection performance. The developed approach does not depend on simulation (Hijkata et al., 2021), estimation methods (Krénusz et al., 2021), model-based (Wu et al., 2023b), or control approaches (Moaveni et al., 2020), although it could be used in combination with such methods to improve the robustness of the detection. Furthermore, the obtained results provided evidence of ability for early detection of slippage phenomena. Early detection is particularly important, as in current anti-slipping control systems, detection is primarily performed on the basis of speed or acceleration differences exceeding pre-determined values, which may lead to false detections or miss opportunities to provide early detection (Yin et al., 2024). This is particularly useful in practice, as there is a time lag between when braking or acceleration are applied, until their effects are observable. Such proactive detection could enable automatic activation of controllers to gently disengage the brakes, moderate the applied acceleration, or deploy additional sanding to mitigate the slip activity.

Therefore, the benefits could be applicable to a significant proportion of operational trains which lack sophisticated anti-slipping control mechanisms, and it could even improve such mechanisms where they are currently installed. In conclusion, the performed comparative experimental evaluation provides evidence for the superior performance of the developed hybrid approach which combines wavelet features with joint LSTM and MLP modelling.

The analysis presented herein nonetheless has some limitations. Although the experiments performed considered comparisons with a range of models, the design of experiments considered a limited range of hyper-parameter settings for the tested approaches. Although the identified by the grid search best hyperparameters were applied in the reported experiments for all employed methods, to optimise performance

Fig. 9. Wheel slip activity during acceleration phase.

based on existing evidence, such performance may vary across a wider range of datasets or sets of models and their hyperparameters. Therefore, results should be seen as evidence, which is indicative, although not conclusive.

Additionally, the data annotation process, which originated from existing operational systems, despite being overseen by subject matter experts, may still be a source of potential errors, thereby influencing subsequent learning and classification results. Notably, the conducted experiments do not accommodate for contextually pertinent parameters such as track and wheel condition, vehicle mass, and traction forces, resulting in a possible performance constraint on the overall analysis. Further work could consider the combined use of approaches such as the one presented in this work with further condition monitoring (Mosleh et al., 2023a), fault detection (Mosleh et al., 2023b), and anti-slip control mechanisms (Yin et al., 2024; Moaveni et al., 2020). Such further work could jointly benefit from data readily available from operational trains, and the benefits of the additional approaches in bringing in more contextual information regarding the status of the rail-wheel interface and the control effects of anti-slipping mechanisms. The presented work, which demonstrates early detection capabilities, is well-aligned with aims to equip trains with predictive monitoring capabilities, which go beyond event detection, and can enhance existing anti-slipping control mechanisms.

Further research could investigate the performance of an LSTM + MLP approach in other complex wheel-rail environments. This should be contingent on several factors, including the quality and coverage of the datasets, the specific architecture and hyperparameters of the model, and the variability in environmental conditions. While such an investigation was beyond the scope of the present study, given the available datasets, further work should involve additional comprehensive datasets that cover a wider range of wheel-rail interactions under various conditions. In such a study it would be of interest to investigate how the architecture can be tailored to the complexity of the problem, and which combination of hyperparameter settings and preprocessing would lead to high performance. The model's ability to generalize to new conditions can be enhanced through methods such as transfer learning and the integration of domain knowledge. Robust evaluation metrics and validation strategies are necessary to ensure reliable performance across different scenarios.

5. Conclusion

This paper presented the development of a novel detection methodology for train wheel sliding for two main types of wheel slip, namely adhesion-limited and traction-limited slip, presenting evidence of high performance with early detection capability. Instead of focusing on theoretical models, simulation, or advanced measurements, the proposed method is based on measurements which can be obtained from actual operational trains, namely brake pressures and train carriage axle speeds. From the end application perspective, the data workflow is organised in four stages: signal acquisition, pre-processing, analysis, and performance assessment. The method was effective in detecting wheel slip activity, achieving higher performance compared to other classification-based machine learning. The analysis was performed over extensive data operating from diesel multiple unit trains over a period of a whole year.

Nonetheless, the suggested approach carries certain limitations such as partial dependence on expert annotations and the limitations linked to the empirical determination and the settings for identifying the best settings for the hyperparameters. The omission of contextual factors, such as weather conditions, track condition, traction load, and wheel conditions in the analysis also curtails the overall performance. Future enhancement efforts could address these identified limitations and integrate additional external data for enhanced diagnostic efficacy. Ultimately, the long-term research direction involves the development of a distributed online diagnostic system with fault isolation capabilities, enabling analogous train systems to share newly discerned fault characteristics. Increased confidence in methods such as the one reported in the present work are a concrete positive step in this direction.

CRediT authorship contribution statement

Bernadin Namoano: Writing – review & editing, Writing – original draft, Visualization, Software, Methodology, Investigation, Data curation, Conceptualization. **Christos Emmanouilidis:** Writing – review & editing, Writing – original draft, Supervision, Methodology, Investigation, Conceptualization. **Andrew Starr:** Writing – review & editing, Supervision, Resources, Funding acquisition, Conceptualization.

Declaration of competing interest

The authors declare that they have no known competing financial interests or personal relationships that could have appeared to influence the work reported in this paper.

Data availability

The data that has been used is confidential.

Acknowledgments

The authors wish to thank Unipart Rail, Instrumentel for providing the industrial data and domain-specific expertise and the Engineering and Physical Sciences Research Council (EPSRC) for the financial support through grant 2203091.

References

Abouzeid, A.F., Trimpe, F.F., Lück, S., Traupe, M., Guerrero, J.M., Briz, F., 2022. Co-Simulation-Based verification of torsional vibration protection of electric-driven railway vehicle wheelsets. Vibrations 5 (3), 613–627. https://doi.org/10.3390/vibration5030036.

Barna, G., 2011. Control system of wheel slide protection devices for rail vehicles meeting the requirements of European normative documents system sterowania układów. In: Proceedings of 13th International Conference on Quality, Safety and Ecology in Transport, pp. 11–18.

Bosso, N., Gugliotta, A., Magelli, M., Oresta, I.F., Zampieri, N., 2019. Study of wheel-rail adhesion during braking maneuvers. Procedia Struct. Integr. 24, 680–691. https://doi.org/10.1016/j.prostr.2020.02.060.

Charles, G., Goodall, R., Dixon, R., 2008. Model-based condition monitoring at the wheel-rail interface. Veh. Syst. Dyn. 46 (Suppl. 1), 415–430. https://doi.org/10.1080/00423110801979259.

Daugman, J.G., 1985. Uncertainty relation for resolution in space, spatial frequency, and orientation optimized by two-dimensional visual cortical filters. J. Opt. Soc. Am. 2 (7), 1160. https://doi.org/10.1364/josaa.2.001160.

Deng, X., Ni, Y.-Q., Liu, X., 2022. Numerical analysis of transient wheel-rail rolling/slipping contact behaviors. J. Tribol. 144 (10) https://doi.org/10.1115/1.4054592.

EN 15595, 2021. Railway Applications—Braking—Wheel Slide Protection.

Enblom, R., 2009. Deterioration mechanisms in the wheel-rail interface with focus on wear prediction: a literature review. Veh. Syst. Dyn. 47 (6), 661–700. https://doi.org/10.1080/00423110802331559.

Garnham, J.E., Davis, C.L., 2009. Rail materials. In: Wheel-Rail Interface Handbook. Elsevier, pp. 125–171. https://doi.org/10.1533/9781845696788.1.125.

Hijkata, D., Kizaki, Y., Nakazawa, S., 2021. A hybrid simulator for wheel slide protection combining pneumatic brake hardware and a real-time computer. The Proceedings of the Transportation and Logistics Conference 30 (0), 1–4. https://doi.org/10.1299/jsmetld.2021.30.SS1-1-4, 2021.

Hochreiter, S., Schmidhuber, J., 1997. Long short-term memory. Neural Comput. 9 (8), 1735–1780. https://doi.org/10.1162/neco.1997.9.8.1735.

Ishige, M., 2021. Recent activities in vehicle technology research and development. Quarterly Report of RTRI 62 (1), 1–5. https://doi.org/10.2219/rtriqr.62.1_1.

Iwnicki, S., 2006. In: Iwnicki, S., Iwnicki, S. (Eds.), Handbook of Railway Vehicle Dynamics. CRC Press. https://doi.org/10.1201/9781420004892.

Keogh, E., Ratanamahatana, C.A., 2005. Exact indexing of dynamic time warping. Knowl. Inf. Syst. 7 (3), 358–386. https://doi.org/10.1007/s10115-004-0154-9.

Krénusz, M., Kovács, R.S., Krémer, M., 2021. Estimating the damage of railway carriage wheels equipped with disc brakes. Period. Polytech. - Mech. Eng. 65 (3), 286–292. https://doi.org/10.3311/PPme.18099.

Krummenacher, G., Ong, C.S., Koller, S., Kobayashi, S., Buhmann, J.M., 2018. Wheel defect detection with machine learning. IEEE Trans. Intell. Transport. Syst. 19 (4), 1176–1187. https://doi.org/10.1109/TITS.2017.2720721.

Lewis, R., Olofsson, U., 2009. Wheel—rail Interface Handbook. Woodhead Publishing Limited. https://doi.org/10.1533/9781845696788.

Lu, C., Chen, D., Shi, J., Li, Z., 2024. Research on wheel-rail dynamic interaction of high-speed railway under low adhesion condition. Eng. Fail. Anal. 157 https://doi.org/10.1016/j.engfailanal.2023.107935.

Lukoševičius, M., Jaeger, H., 2009. Reservoir computing approaches to recurrent neural network training. Computer Science Review 3 (3), 127–149. https://doi.org/10.1016/j.cosrev.2009.03.005.

Maglio, M., Vernersson, T., Nielsen, J.C.O., Pieringer, A., Söderström, P., Regazzi, D., Cervello, S., 2022. Railway wheel tread damage and axle bending stress – instrumented wheelset measurements and numerical simulations. Int. J. Real. Ther. 10 (3), 275–297. https://doi.org/10.1080/23248378.2021.1932621.

Misiti, M., Oppenheim, G., Poggi, J.-M., Misiti, Y., 2006. Wavelets and Their Applications (Digital Signal and Image Processing Series). ISTE.

Moaveni, B., Fathabadi, F.R., Molavi, A., 2020. Supervisory predictive control for wheel slip prevention and tracking of desired speed profile in electric trains. ISA (Instrum. Soc. Am.) Trans. 101, 102–115. https://doi.org/10.1016/j.isatra.2020.01.011.

Mosleh, A., Meixedo, A., Ribeiro, D., Montenegro, P., Calçada, R., 2023a. Automatic clustering-based approach for train wheels condition monitoring. Int. J. Real. Ther. 11 (5), 639–664. https://doi.org/10.1080/23248378.2022.2096132.

Mosleh, A., Meixedo, A., Ribeiro, D., Montenegro, P., Calçada, R., 2023b. Early wheel flat detection: an automatic data-driven wavelet-based approach for railways. Veh. Syst. Dyn. 61 (6), 1644–1673. https://doi.org/10.1080/00423114.2022.2103436.

Namoano, B., Ruiz-Carcel, C., Emmanouilidis, C., Starr, A.G., 2022. Data-driven wheel slip diagnostics for improved railway operations. ELSEVIER, IFAC-PapersOnLine 55 (19), 103–108. https://doi.org/10.1016/j.ifacol.2022.09.191.

Nicks, S., 1998. Condition monitoring of the track/train interface. In: IEE Seminar Condition Monitoring for Rail Transport Systems, p. 7. https://doi.org/10.1049/ic:19980980, 7.

Pascanu, R., Mikolov, T., Bengio, Y., 2012. On the difficulty of training recurrent neural networks. In: 30th International Conference on Machine Learning, ICML 2013, PART, vol. 3, pp. 2347–2355.

Pugi, L., Paolieri, G., Giorgetti, M., Berzi, L., Viviani, R., Cabrucci, L., Bocciolini, L., 2023. HIL testing of wheel slide protection systems: criteria for continuous updating and validation. Railway Engineering Science 31 (2), 108–121. https://doi.org/10.1007/s40534-022-00298-7.

The Rail Delivery Group, 2018. Managing Low Adhesion, sixth ed. https://www.raildeliverygroup.com/media-centre-docman/121-2018-01-managing-low-adhesion-ed6-0/file.html.

UIC, 2005. In: UIC Code 541-5 - Brakes - Specifications for the Construction of Various Brake Parts - Wheel Slide Protection Device (WSP), third ed.

Wu, Q., Cole, C., Spiryagin, M., Chang, C., Wei, W., Ursulyak, L., Shvets, A., Murtaza, M. A., Mirza, I.M., Zhelieznov, K., Mohammadi, S., Serajian, H., Schick, B., Berg, M., Sharma, R.C., Aboubakr, A., Sharma, S.K., Melzi, S., Di Gialleonardo, E., et al., 2023a. Freight train air brake models. Int. J. Real. Ther. 11 (1), 1–49. https://doi.org/10.1080/23248378.2021.2006808.

Wu, Q., Cole, C., Spiryagin, M., Chang, C., Wei, W., Ursulyak, L., Shvets, A., Murtaza, M. A., Mirza, I.M., Zhelieznov, K., Mohammadi, S., Serajian, H., Schick, B., Berg, M., Sharma, R.C., Aboubakr, A., Sharma, S.K., Melzi, S., Di Gialleonardo, E., et al., 2023b. Freight train air brake models. Int. J. Real. Ther. 11 (1), 1–49. https://doi.org/10.1080/23248378.2021.2006808.

Yang, Y., Ling, L., Wang, J., Zhai, W., 2023. A numerical study on tread wear and fatigue damage of railway wheels subjected to anti-slip control. Friction 11 (8), 1470–1492. https://doi.org/10.1007/s40544-022-0684-8.

Yin, S., Peng, T., Yang, C., Yang, C., Chen, Z., Gui, W., 2024. Dynamic hybrid observer-based early slipping fault detection for high-speed train wheelsets. Control Eng. Pract. 142 https://doi.org/10.1016/j.conengprac.2023.105736.

Zirek, A., Onat, A., 2020. A novel anti-slip control approach for railway vehicles with traction based on adhesion estimation with swarm intelligence. Railway Engineering Science 28 (4), 346–364. https://doi.org/10.1007/s40534-020-00223-w.

https://dspace.org/

Detecting wheel slip from railway operational data through a combined wavelet, long short-term memory and neural network classification method

Namoano, Bernadin; Emmanouilidis, Christos; Starr, Andrew

2024-11
Elsevier
https://doi.org/10.1016/j.engappai.2024.109173
Namoano B, Emmanouilidis C, Starr A. (2024) Detecting wheel slip from railway operational data through a combined wavelet, long short-term memory and neural network classification method. Engineering Applications of Artificial Intelligence, Volume 137, Part B, November 2024, Article number 109173

Downloaded from a DSpace repository. https://dspace.org/